Comprehensive study of crystallization and phase formation in (La,Gd)BGeO$_5$ glass

Yoshihiro TAKAHASHI,[†] Yasuhiko BENINO,[*] Takumi FUJIWARA and Takayuki KOMATSU[**]

Department of Applied Physics, Tohoku University, 6−6−05, Aoba, Aoba-ku, Sendai, Miyagi 980−8579
[*]Graduate School of Environmental Science, Okayama University, 3−1−1, Tsushimanaka, Okayama 700−8530
[**]Department of Materials Science and Technology, Nagaoka University of Technology,
  1603−1, Kamitomioka-cho, Nagaoka, Niigata 940−2188

The glasses with $(25-x)$La$_2$O$_3$·xGd$_2$O$_3$·25B$_2$O$_3$·50GeO$_2$ composition corresponding to the (La,Gd)BGeO$_5$ were prepared, and the substitution effect of gadolinium ions (Gd^{3+}) on crystallization behavior and phase formation was examined by DTA, XRD and Raman techniques in detail. Ferroelectric (La,Gd)BGeO$_5$ phase with hexagonal stillwellite structure were crystallized in the composition range of $x = 0$–15. Although no significant change in physical properties was observed in the whole composition range, crystallization behavior was drastically changed as the progressive substitution of Gd^{3+} was carried out (i.e., crystallization of monoclinic phase of (La,Gd)BGeO$_5$ and high-pressure phase of Gd$_2$Ge$_2$O$_7$ with a triclinic structure). Structure of the glasses and crystallized phases, and the phase formation mechanism were also discussed.

1.　Introduction

Lanthanide-containing inorganic materials, such as crystal, glass and glass-ceramics, have been extensively investigated and developed for application to electric and photonic device materials. In these materials, added/substituted lanthanide (*Ln*) ions play a significant role for their functionalities, e.g. ferroelectricity, fluorescence and laser-oscillation.

LaBGeO$_5$ crystals have a hexagonal stillwellite (CeBSiO$_5$)-type structure, in which BO$_4$ tetrahedra form screw chains along *c*-axis and La ions are in the ninefold vertices arranged under and over slightly distorted GeO$_4$ tetrahedra.[1] The LaBGeO$_5$ crystal is ferroelectric and shows an unique phase-transition behavior.[2]–[5] After demonstration of continuous-wave laser emissions in the green region by self-frequency doubling in Nd^{3+}-doped stillwellite-type LaBGeO$_5$ single crystal,[1],[6] this crystal has received much interest as a novel laser host and nonlinear optical crystal.

Since the LaBGeO$_5$ crystal consists of a *Ln* element and glass-forming oxides (B$_2$O$_3$ and GeO$_2$), this crystal has two specific features, i.e., i) stoichiometric composition of LaBGeO$_5$ crystal, i.e., 25La$_2$O$_3$·25B$_2$O$_3$·50GeO$_2$, easily vitrify and the LaBGeO$_5$ crystalline phase is precipitated by crystallization,[7]–[9] and ii) large quantity of *Ln*$^{3+}$ could be substituted in La^{3+} site of LaBGeO$_5$ crystal.[10] Therefore, many researchers have also had a great interest in "stillwellite-related glass and glass-ceramics" from the viewpoint not only of ferroelectrics, but also of optical material. For example, Verwey et al. investigated luminescent properties and the quantum efficiency of Eu^{3+} in LaBGeO$_5$ glass and compared them with that of Eu^{3+} in LaBGeO$_5$ crystal.[11] In addition, Kaminskii et al. proposed the Nd^{3+}-doped LaBGeO$_5$ glass for a new laser material since pulsed stimulated emission was demonstrated in this glass at room temperature.[12] Takahashi

et al. succeeded in fabricating transparent LaBGeO$_5$-crystallized glasses indicating strong and coherent second-harmonic generation (SHG) for the first time, and investigated the *Ln*-substitution effect on ferroelectric and SHG properties in the stillwellite-type (La,*Ln*)BGeO$_5$ glass-ceramics.[10],[13]–[16] They also demonstrated that the second-order optical nonlinearity of transparent LaBGeO$_5$-crystallized glass, which was obtained by crystallization of the stoichiometric glass, was comparable to that of LaBGeO$_5$ single crystal.[17],[18] Furthermore, recently, Gupta et al. succeeded in drawing optical waveguides consisting of stillwellite-type (La,Nd)BGeO$_5$ and (La,Sm)BGeO$_5$ crystals in the corresponding glasses by laser irradiation.[19],[20]

Thus, the stillwellite-related glass/glass-ceramics have a great potential for advanced photonic devices, i.e., laser host, wavelength conversion and optical integrated circuit. In order to apply these materials to the device components, the *Ln*-substitution effects on physical properties and crystallization behavior is an important issue that we should clarify. Therefore, in this study, we prepared the glasses with composition of $(25-x)$La$_2$O$_3$·xGd$_2$O$_3$·25B$_2$O$_3$·50GeO$_2$, corresponding to the stoichiometry of (La,Gd)BGeO$_5$, and examined their physical properties, crystallization behavior and phase formation for the purpose of comprehensive understanding of the *Ln*-substitution effects in the LaBGeO$_5$ glass. In this study, gadolinium oxide, Gd$_2$O$_3$, was chosen as a substitution substance in the LaBGeO$_5$ glass since introduction of gadolinium ions (Gd^{3+}) into the glass do not disturb the optical and spectroscopic measurements due to the absence of optical absorption band in visible region.

2.　Experimental

2.1　Sample preparation

The glass compositions examined in the present study was $(25-x)$La$_2$O$_3$·xGd$_2$O$_3$·25B$_2$O$_3$·50GeO$_2$ ($x = 0$–25), which correspond to the stoichiometry of (La,Gd)BGeO$_5$. The bulk glasses were prepared by a conventional melt-quenching method.

[†]　Corresponding author: Y. Takahashi; E-mail: takahashi@laser.apph.tohoku.ac.jp

Commercial powders of reagent grade La_2O_3 (99.9%), Gd_2O_3 (99.9%), B_2O_3 (99.9%) and GeO_2 (99.95%) were thoroughly mixed and ground in an alumina mortar. The batch weight was 40 g. The mixtures were melted in a platinum crucible with a lid at 1300–1350°C for 20 min in an electric furnace. The melts were poured onto an iron plate heated at ~300°C and pressed to a thickness of about 1.5 mm.

2.2 Characterization

Crystallization behaviors and thermal parameters, glass transition, T_g, crystallization on-set, T_x, and crystallization peak, T_p, temperatures were examined by a differential thermal analysis (DTA) at a heating rate of 10 K/min. The glassy state in the melt-quenched samples, the crystalline phases present in the heat-treated glasses and the lattice constants were examined by an X-ray diffraction (XRD) analysis using Cu Kα radiation. Density of the glass samples was determined using the Archimedes, method with distilled water as an immersion liquid. Refractive index at 587.6 nm (He-D line) was measured using the V-block prism, which was made from the large bulk glass, with dimension of ~3 × 3 × 1 cm by a precision refractometer (Kalnew, KPR–200 Model). Raman spectra of the as-quenched glasses and crystallized phases were measured using an Ar$^+$ laser operating at 514.5 nm. The scattered light was detected using the system consisting of a triple grating monochrometer and a liquid-nitrogen-cooled CCD device detector (HORIBA-Jobin Yvon, T64000). All of the measurements were done at room temperature.

3. Results

3.1 Physical property

Transparent and colorless melt-quenched samples were successfully fabricated in the whole composition range. The all samples showed a halo pattern in the XRD patterns, which indicated the amorphous nature of the samples. The values of density, d, and refractive index at 587.6 nm (He-D line), n_d, of the (La,Gd)BGeO$_5$ glasses studied are summarized in **Table 1**. The d and n_d were present in the range of ~5.0–5.5 g/cm^3 and ~1.81–1.80, respectively. The increases in d and slight decrease in n_d were observed as progressive substitution of Gd^{3+} was carried out. The values of molar volume, V_m, and molar polarizability, α_m, which is calculated by the Lorentz–Lorenz equation,[21] are also given in Table 1.

3.2 DTA study

Figure 1 shows the DTA curves in (25–x)La$_2$O$_3$·xGd$_2$O$_3$·25B$_2$O$_3$·50GeO$_2$ glasses fabricated in this study. Pulverized glasses were used in the DTA study because the pure and Gd-substituted LaBGeO$_5$ glasses revealed strong tendency of surface-crystallization.[13]–[15] The glass transition, crystallization on-set, and first crystallization peak temperatures were estimated to be T_g = 673–715°C, T_x = 806–843°C and T_p = 824–866°C, respectively. Although only one crystallization peak was observed in the case of x = 0–5, in the glass with x = 10, an additional exothermic peak appeared at T_{p2} = 1108°C, just below the melting temperature (1144°C). Increasing the substitution amount (x), the T_{p2} shifted to lower temperature, and eventually, the T_{p2} apparently overlapped the T_{p1}, and another crystallization peak emerged at 1053°C in the x = 25 (corresponding to GdBGeO$_5$ composition). The thermal parameters of (La,Gd)BGeO$_5$ glasses are also summarized in Table 1.

3.3 XRD study

The powder XRD patterns of the (La,Gd)BGO glasses heat-treated at T_{p1} for 5 h are shown in **Fig. 2**. In the heat-treated glass samples with x = 0–15 (i.e., LaBGeO$_5$ to La$_{0.4}$Gd$_{0.6}$BGeO$_5$ composition), these XRD patterns are assigned to the stillwellite phase by comparison of the crystallographic data of LaBGeO$_5$ (JCPDS: 41–659). In the case of x = 10–15, the diffraction intensity of crystallized phases decreased with increasing the x, and an unidentified peak was observed around 2θ = 28°.

Figure 3 shows the lattice constants and density of the stillwellite phase with a hexagonal structure crystallized in the glasses. The density of stillwellite phases was estimated from the lattice constants of stillwellite-type (La,Gd)BGeO$_5$ and their molecular weight. The density of the (La,Gd)BGeO$_5$ glasses (d in Table 1) are also included. The lattice constants of stillwellite-type LaBGeO$_5$ crystallized in the corresponding glass (x = 0) were evaluated to be a = 0.6989 nm and c = 0.6860 nm. These value well corresponded to the values in the JCPDS card, i.e., a = 0.69923 nm and c = 0.68631 nm. It is seen that the lattice constants of the a- and c-axes decrease systematically with increasing the Gd$_2$O$_3$ content, according to Vegard's rule. The density of stillwellite phases (opened square) increased by approximately five percent compared to that of corresponding glasses (closed square).

The powder XRD patterns of the glass samples with x = 10–15 heat-treated around each T_{p2} for 5 h are shown in **Fig. 4**. These XRD patterns indicated more complicate patterns compared to

Table 1. Density d, Refractive Index at 587.6 nm (He-D Line), n_d, Molar Volume, V_m, Molar Polarizability α_m, Glass Transition, T_g, Crystallization Onset, T_x, Crystallization Peak, T_p, and Melting, T_m, Temperatures, in (25–x)La$_2$O$_3$·xGd$_2$O$_3$·25B$_2$O$_3$·50GeO$_2$ Glasses

x	density/ gcm^{-1}	n_d	V_m/cm^{3}mol^{-1}	α_m/Å^3	T_g/°C	T_x/°C	T_{p1}/°C	T_{p2}/°C	T_m/°C	phase around T_{p1}	phase around T_{p2}
0	4.957	1.8150	30.49	5.239	673	808	824	–	1194	*stil.**	–
2.5	5.045	1.8175	30.14	5.190	678	806	824	–	1158	*stil.*	–
5	5.100	1.8162	30.00	5.159	684	811	830	–	1159	*stil.*	–
10	5.195	1.8120	29.80	5.106	692	827	843	1108	1144	*stil.*	*mono.* ?
13	5.262	1.8110	29.63	5.073	693	831	870	1083	1137	*stil.*	*mono.* **
15	5.313	1.8115	29.48	5.050	698	829	856	1006	1146	*stil.*	*mono.*
20	5.452	1.8055	29.07	4.952	708	843	868	911	1175	β'-Gd$_2$Ge$_2$O$_7$	*mono.*
25	5.520	1.8055	29.04	4.947	715	841	866	1053	>1200	β'-Gd$_2$Ge$_2$O$_7$, *unkn.****	*mono.*

stil. : stillwellite phase.
**mono.* : monoclinic phase.
***unkn.* : unknown phase (*A phase*).
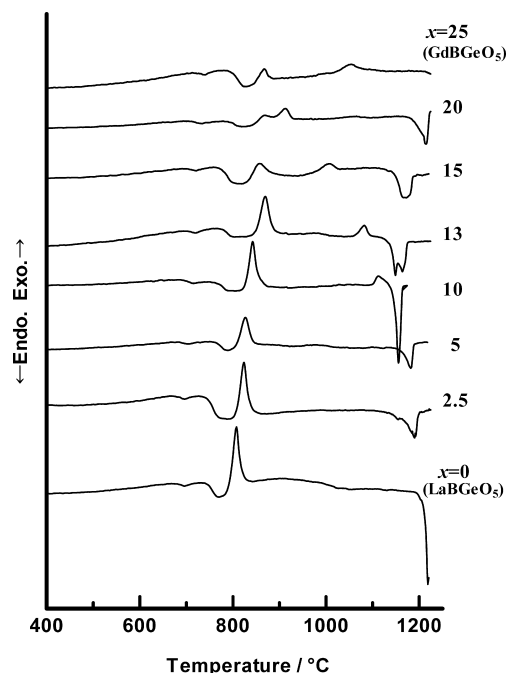
Fig. 1. DTA curves of (25–x)La₂O₃·xGd₂O₃·25B₂O₃·50GeO₂ glasses. Heating rate was 10 K/min.
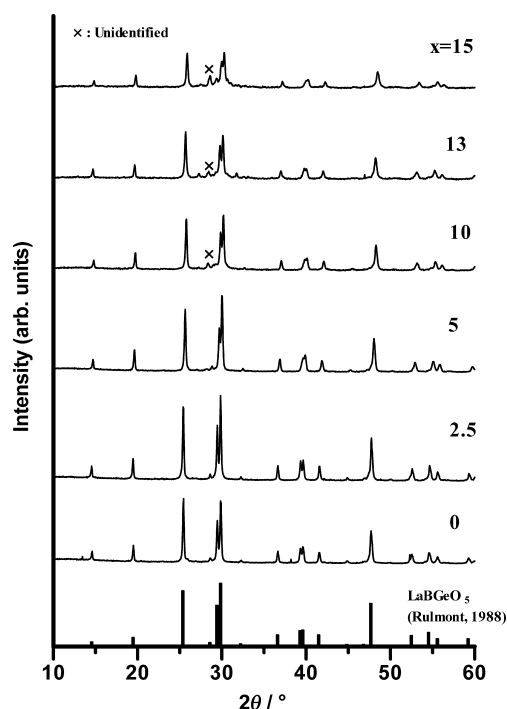
Fig. 2. Powder XRD patterns of (La,Gd)BGO crystallized glasses obtained by heat-treatment at T_p for 5 h.
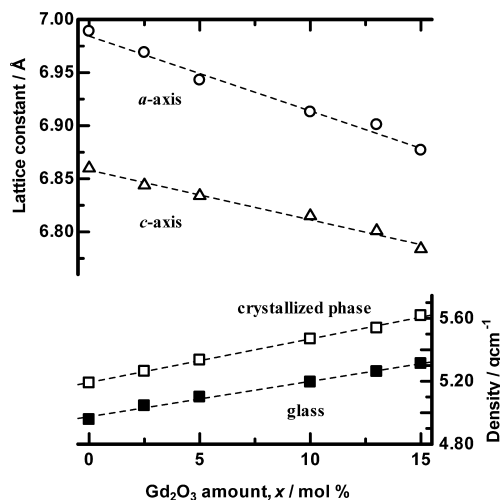

Fig. 3. Lattice constants and density of the stillwellite-type phases crystallized in the (La,Gd)BGeO₅ glasses.

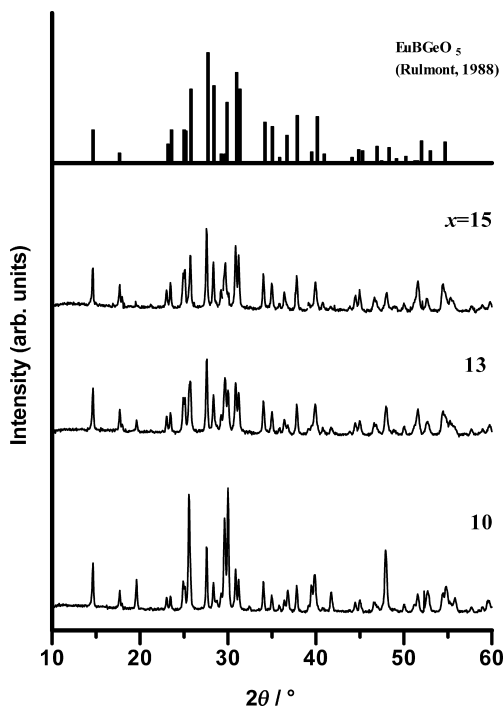Fig. 4. Powder XRD patterns of the glass samples with x = 10–15 heat-treated around T_{p2} for 5 h.

those of stillwellite phases seen in Fig. 2. In the glass with x = 13 and 15, great similarity of XRD patterns to that of the monoclinic LnBGeO₅ compounds were confirmed by comparison to XRD data of monoclinic phase. The data of EuBGeO₅ is included in Fig. 4 as a representative of monoclinic phase because the mean ionic radius of Ln^{3+} in the glass with x = 15 (0.1290 nm) is close to the radius of Eu³⁺ (0.1260 nm).[22] Although the XRD pattern of the crystallized glass with x = 10 was

correspondent to neither stillwellite-type nor monoclinic-type, both features of stillwellite and monoclinic phases were confirmed.

With regard to the glasses with x = 20 and 25, their crystallization behavior was different from those of the glasses with x = 0–15: **Figure 5** shows the powder XRD patterns of the glass sample with x = 20 heat-treated near T_{p1} and T_{p2} for 5 h. Since the position of T_{p1} (868°C) was relatively close to that of T_{p2} (912°C) in this glass, the following heat-treatment temperatures were chosen in order to crystallize the glass with x = 20 into the phases corresponding to the T_{p1} and T_{p2}, separately, i.e., 838°C (T_{p1}–30°C) and 930°C (higher than T_{p2}). Unlike the case of the glasses with x = 0–15 heat-treated at ~T_{p1}, more complicate XRD pattern was found after crystallization around T_{p1}, instead of the stillwellite phase. The XRD pattern of crystallized phase indi-
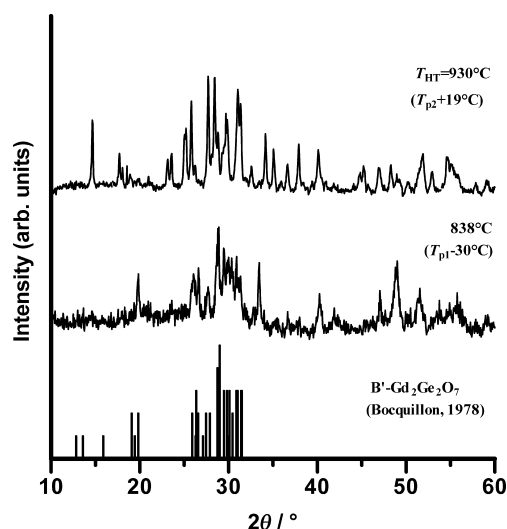
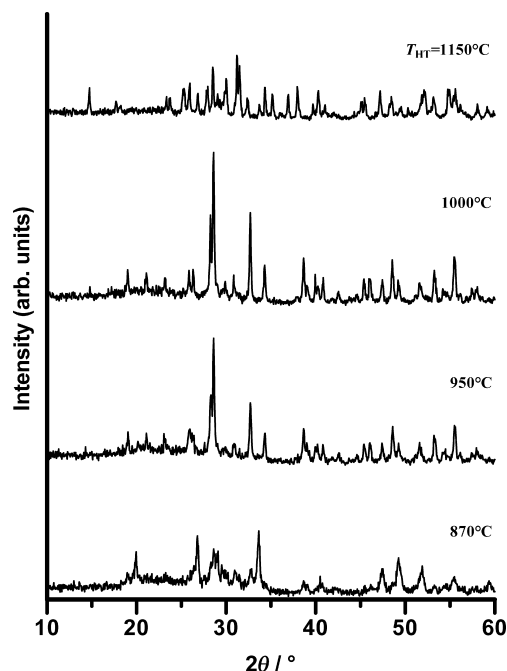Fig. 5.   Powder XRD patterns of the glass sample with $x = 20$ heat-treated near T_{p1} and T_{p2} for 5 h.

Fig. 6.   Powder XRD patterns of glass sample with $x = 25$ (GdBGeO$_5$ composition) heat-treated at various temperatures for 5 h.
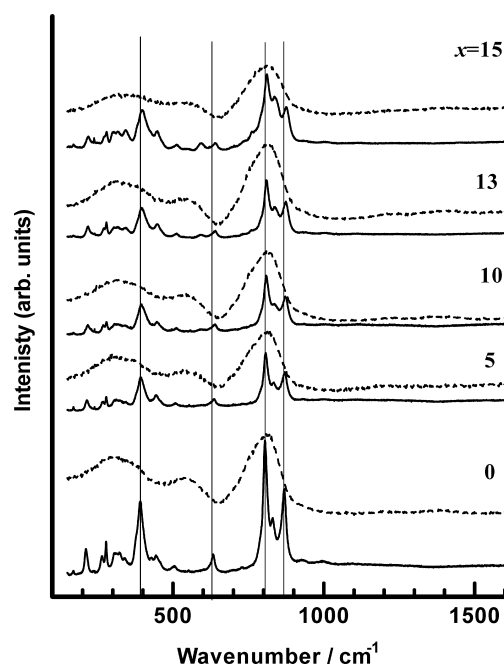

Fig. 7.   Raman scattering spectra of the as-quenched (dashed line) with $x = 0$–15 and the crystallized glasses obtained at T_{p1} for 5 h (solid line).
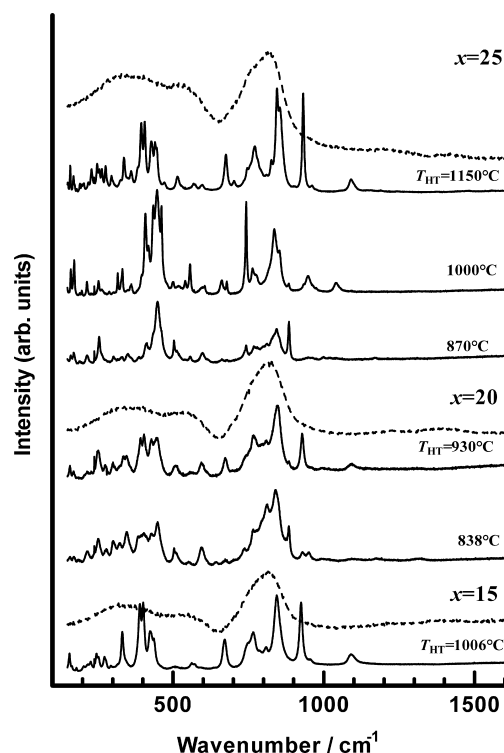

Fig. 8.   Raman scattering spectra of the as-quenched (dashed line) with $x = 15$–25 and the crystallized glasses obtained at various temperatures for 5 h (solid line).

cated the great similarity to that of B'-Gd$_2$Ge$_2$O$_7$, which was a high-pressure phase in Gd$_2$Ge$_2$O$_7$ (JCPDS: 34–1168), whereas the monoclinic phase was crystallized at 930°C.

The powder XRD patterns of the glass sample with $x = 25$, i.e., GdBGeO$_5$, heat-treated at various temperatures are shown in **Fig. 6**. In here, four temperatures were selected as crystallization condition, i.e., 870°C (~T_{p1}) for 5 h, and 950°C, 1000°C and 1150°C (higher than T_{p2}) for 3 h. The XRD pattern of the glass heat-treated near T_{p1} was almost identical with that of crystallized phase in the glass with $x = 20$ around T_{p1}. In addition, the XRD pattern of phase crystallized at 1150°C could be assigned to the monoclinic phase. However, in the glasses heat-treated at 950°C and 1000C°, the XRD pattern was quite different from the phases formed at either around T_{p1} or T_{p2}., i.e., B'-Gd$_2$Ge$_2$O$_7$ and

monoclinic phases. Since the crystalline phase could not be assigned to any phases reported so far, this phase is hereafter called as "*A phase*" in this paper for the sake of convenience.

3.4   Raman scattering spectra
Figures 7 and **8** show the Raman scattering spectra of the as-

quenched (dashed line) and crystallized glasses (solid line) with $x = 0$–15 and $x = 15$–25, respectively. All of the glasses indicated the broadened bands, which were characteristic of amorphous state, mainly around 800–900 cm^{-1}, 500–600 cm^{-1}, and 300–400 cm^{-1}. On the other hand, after crystallization of (La,Gd)BGeO₅ glasses with $x = 0$–15 at T_{p1} for 5 h, the Raman spectra showed very sharp bands, indicating transformation from amorphous to crystal state. The Raman bands were mainly observed at 800–900 cm^{-1}, ~630 cm^{-1} and 350–450 cm^{-1}. These spectra measured in this study indicated considerable similarity to that of LaBGeO₅ phase reported by Rulmont and Tarte.[23] Although the Raman spectra were almost identical in the crystallized glasses with $x = 0$–15, the Raman scattering intensity was decreased by the substitution of Gd^{3+} (i.e., the increase in x).

As seen in Fig. 8, the complicate Raman spectrum, implying lower symmetry of the crystal structure, was obtained in the glass with $x = 15$ annealed at T_{p2} (1006°C) for 5 h, as well as the results from XRD study. Fine and sharp Raman peaks were observed at ~1100 cm^{-1}, 650–950 cm^{-1} and 300–450 cm^{-1}. The similar spectra also could be confirmed in the glasses with $x = 20$ and 25 annealed around T_{p2}. These Raman spectra have great similarities to that of monoclinic GdBGeO₅. Particularly, the crystallized phase from the glass with $x = 25$, i.e., stoichiometry of GdBGeO₅, showed completely same Raman spectrum of monoclinic GdBGeO₅.[23] Furthermore, the spectra of phases crystallized around T_{p1} in the glasses with $x = 20$ and 25 were different from those of stillwellite- and monoclinic-types, and the distinct Raman peak could not be detected at ~1100 cm^{-1} in the spectra.

4.   Discussion

4.1   Physical property of (La,Gd)BGeO₅ glasses

The increase in density, d, and the decrease in molar volume, V_m, were confirmed by the substitution of Gd^{3+} for La^{3+} in the (La,Gd)BGeO₅ glasses. These are probably due to the introduction of Gd^{3+} with a larger atomic number and smaller ionic radius than La^{3+}. On the contrary, the n_d and α_m tended to decrease with increasing the x. This implies that the Gd^{3+} has a small polarizability compared to the La^{3+}. The decrease in refractive index with decreasing the ionic radius of Ln^{3+} is also confirmed in the Ln_2O_3–GeO₂ and Ln_2O_3–TiO₂–GeO₂ glass systems.[24]

4.2   Crystallization and phase formation in (La,Gd)BGeO₅ glass

Although the (La,Gd)BGeO₅ glasses did not show any remark-

Fig. 9.   Schematic picture of phase formation in (La,Gd)BGeO₅ glasses.

able changes in the physical properties, the drastic change in crystallization behavior was confirmed as the progressive substitution of Gd^{3+} was carried out: **Figure 9** shows the schematic picture of phase formation in the (La,Gd)BGeO₅ glasses based on the DTA, XRD and Raman results in this study. From this map, one can notice the following features about the phase formation;

(1)   The stillwellite phases crystallized in the large composition range ($x = 0$–15)

(2)   In higher Gd-containing glasses ($x = 10$–15), the monoclinic phases crystallized after formation of the stillwellite phase.

(3)   Further increasing the x, B'-Gd₂Ge₂O₇ and unknown phases appeared instead of the stillwellite phase.

4.2.1   Stillwellite-type phase

Crystallization of stillwellite phase in the $(25-x)$La₂O₃·xGd₂O₃·25B₂O₃·50GeO₂ glasses was clarified in the range of $x = 0$–15 by the XRD and Raman studies. It is seen that the lattice constants decrease with the increase of x in accordance with Vegard's rule. In addition, the shift of Raman peaks to higher wavenumber with the substitution of Gd^{3+} was also confirmed. According to the spectroscopic study of stillwellite LaBGeO₅ and monoclinic GdBGeO₅ phases by Rulmont and Tarte,[23] the Raman bands appeared at 800–900 cm^{-1} and ~630 cm^{-1}, and 350–450 cm^{-1} are assigned to the symmetric stretching vibration of BO₄ and GeO₄ tetrahedra, and the bending vibration mode of GeO₄ tetrahedra, respectively. Since the GeO₄ tetrahedral units connect with the La^{3+} in the case of stillwellite phase,[1] the Raman peak shift observed in the stillwellite phases crystallized in (La,Gd)BGeO₅ glasses is probably due to the introduction of Gd^{3+} with higher field strength (i.e., Z/a^2; Z: charge of cation, a: distance between cation and anion, Gd^{3+} and O^{2-} in this case) relative to the La^{3+}. Therefore, from the results of both lattice constant and Raman spectra, it is expected that the substituted Gd^{3+} is substitutionally incorporated into the crystal structure, i.e., formation of the stillwellite-type (La,Gd)BGeO₅.

In the $x = 10$–15, the decrease in peak intensities of XRD and Raman bands was confirmed, implying the reduction of crystallinity. In addition, the unidentified peak was detected at 2θ~28°. In LnBGeO₅ borogermanates, the hexagonal stillwellite phases are obtained for Ln = La to Pr, and Nd (low-temperature phase), and the monoclinic phases are obtained for Ln = Nd (high-temperature phase), Sm to Er and Y with small ionic radii by a solid-state reaction.[23] It means that the ionic radius of Gd^{3+} is too small to crystallize the stillwellite phase. Consequently, it is considered that smallness of ionic radius of Gd^{3+} leads to the deterioration of crystallinity, and formation of the unidentified phase involving Gd₂O₃, which could not be incorporate into the stillwellite phases, in the substitution range of $x = 10$–15.

The increase in density of stillwellite phases obtained by crystallization of the (La,Gd)BGeO₅ glasses is attributed to the rearrangement of glass structure and the decrease in its free volume. In addition, difference of density between the crystallized stillwellite phases and the corresponding glasses was about 5% in the composition range of $x = 0$–15. This result implies that substitution of Gd^{3+} for La^{3+} gives no significant change into the structure of (La,Gd)BGeO₅ glasses. In fact, the Raman spectra of (La,Gd)BGeO₅ were almost identical in the whole composition range. According to Ref. 25, the Raman band observed around 800–900 cm^{-1}, 500–600 cm^{-1}, and 300–400 cm^{-1} are attributed to the antisymmetric stretching of BO₄ and GeO₄ tetrahedra, the bending vibrations of T–O–T (T: B or Ge) bonds, and the La–O vibration, respectively. This indicates that the structural units of (La,Gd)BGeO₅ glasses is very close to that of stillwelite-type
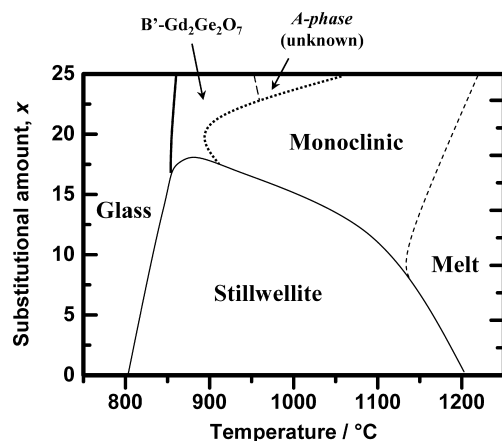
phases. Therefore, it is strongly suggested that there is a considerable structural similarity between the crystallized phases and the corresponding glasses in the scale of short/medium-range order. Such structural similarity of the corresponding glass to the crystallized phase is also reported in other germanate systems.[26),27)]

4.2.2 Monoclinic-type phase

Although the stillwellite and monoclinic phases consist of the tetrahedral BO_4 and GeO_4 units, the crystal structures are quite different from each other: **Figure 10** shows the crystal structure of stillwellite and monoclinic phases. The structure of monoclinic phase has the great similarity to that of datoite, $CaBSiO_4(OH)$, i.e., the layered sheets, in which the BO_4 and GeO_4 tetrahedra are orderly distributed.[28)] Space group of the monoclinic phase in LnBGeO$_5$ compound is $P2_1/a$ (centrosymmetry),[28)] meaning that the monoclinic phase possesses no ferroelectricity and SHG.

The XRD pattern of glass with $x = 10$ heat-treated near T_{p2} (1108°C), which was much higher than the T_{p1} (843°C) corresponding to the crystallization of stillwellite phase, revealed both stillwellite- and monoclinic-type features. This suggests that the T_{p2} was temperature, at which the stillwellite phase transforms to monoclinic one. In addition, it was also confirmed that the monoclinic phase tended to crystallize at lower temperature when the Gd-substitution was progressively carried out. As described above, the monoclinic-type LnBGeO$_5$ crystallizes in the case of Ln = Nd-Er and Y, which have smaller ionic radii than La^{3+}. Particularly, in the case of Ln = Nd, the stillwellite-type and monoclinic-type phases exist as the low- and high-temperature phase, respectively.[23)] These mean that the smaller the ionic radius of Ln becomes, the more stable the monoclinic-type is thermodynamically. Therefore, it is considered that the progressive substitution of Gd^{3+} leads to decrease in the mean ionic radius of lanthanide in the (La,Gd)BGeO$_5$ glasses and consequently, the T_{p2}, which corresponds to the stillwellite-monoclinic phase (that is, low-temperature-high-temperature phase) transition temperature, shifts to lower temperature, i.e.,

$$(La,\text{Gd})\text{BGeO}_5 \text{ (stillwellite-type)}, T < T_{p2}$$
$$\rightarrow (La,\text{Gd})\text{BGeO5 (monoclinic-type)}, T-T_{p2}$$
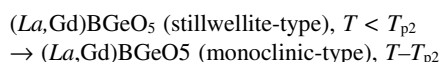
As seen in Fig. 10, the stillwellite-type LaBGeO$_5$ consists of BO$_4$ unit without non-bridging oxygen (NBO) and GeO$_4$ unit with two NBO. On the other hand, the monoclinic GdBGeO$_5$ consists of BO$_4$ and GeO$_4$ units with one NBO. Although the monoclinic phases crystallized in the glasses with $x = 15$–25
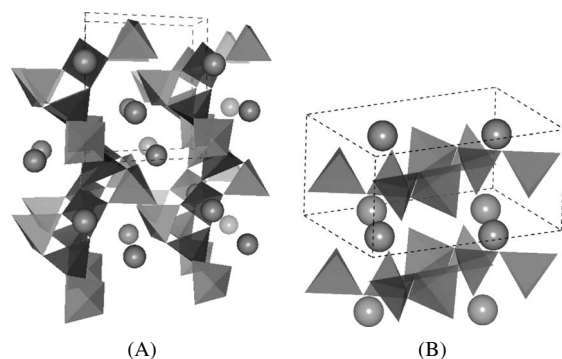

(A)   (B)

Fig. 10. Crystal structures of (A) stillwellite and (B) monoclinic phases in LnBGeO$_5$ compounds. The dotted line indicates unit cell. Sphere, and polyhedra of bright and dark colors correspond to Ln^{3+}, and GeO$_4$ and BO$_4$ tetrahedral units, respectively.

showed the Raman bands at ~1100 cm^{-1} (Fig. 9), such band could not be detected in the stillwellite phases (Fig. 8). It is clearly indicated that the Raman band around 1100 cm^{-1} is due to the presence of tetrahedral BO$_4$ unit with NBO. Although the Raman bands around 700–900 cm^{-1} corresponding to the antisymmetric stretching mode of Ge–O–Ge and stretching mode of Ge–O$^-$ were observed,[29),30)] the band around 1100 cm^{-1} could not be detected in the glasses with $x = 10$–25, which crystallized the monoclinic phases. Therefore, it is deduced that the Ln^{3+} more predominantly bonds to the GeO$_4$ unit than the BO$_4$ unit in (La,Gd)BGeO$_5$ glasses and thus, this is the reason why the first crystallized phase is not the monoclinic phase, but the stillwellite and B'-Gd$_2$Ge$_2$O$_7$ phases in the glasses with $x = 10$–15 and $x = 20$–25, respectively.

4.2.3 High-pressure B'-Gd$_2$Ge$_2$O$_7$ phase

According to Bocquillon et al., there are four types of structure in Gd$_2$Ge$_2$O$_7$ compound, that is, X-, B'-, H- and P-phases.[31)] Whereas the X-phase (tetragonal) crystallized at an ambient pressure, the B'-(triclinic), H-(crystal system is unknown) and P-phases (cubic) crystallized under high pressure of approximately 1.5–4 GPa, 4–5 GPa and 5.8 GPa, respectively.[31)] The XRD patterns of crystalline phases obtained by heat-treatment near the T_{p1} in the glasses with $x = 20$ and 25 indicated the great similarity to that of B'-Gd$_2$Ge$_2$O$_7$ with a triclinic structure by comparison of the crystallographic data (JCPDS: 34–1168). In addition, the crystallized phases in both glasses show the complicated Raman spectra, which reflect the low-symmetry. Therefore, these crystallized phases are considered to be the high-pressure phase of B'-Gd$_2$Ge$_2$O$_7$. This result also indicates that crystallization process of glass has a potential to synthesize the crystalline phase, which could not be obtained by a conventional solid-state reaction, i.e., metastable and high-pressure phases. For example, metastable K$_2$(Nb$_{1/3}$Te$_{2/3}$)$_2$O$_{4.8}$ phase is formed only through crystallization of glass in K$_2$O–Nb$_2$O$_5$–TeO$_2$ system.[32)]

Although the crystal structure of B'-Gd$_2$Ge$_2$O$_7$ phase belongs to triclinic-system, its space group is not described in the JCPDS card (34–1168). Therefore, confirmation of SHG was attempted by means of Kurtz (powder) technique[33)] in the B'-Gd$_2$Ge$_2$O$_7$ phase obtained from the glass with $x = 25$. As a results, the second-harmonic (SH) intensity was approximately 0.15 times compared to that of pulverized α-quartz, i.e., $I_{2\omega}/I_{2\omega, \alpha\text{-quartz}}$~0.15, suggesting that the crystal structure of B'-Gd$_2$Ge$_2$O$_7$ phase is noncentrosymmetry, that is, $P1$.

4.2.4 A phase (unknown phase)

The crystalline phases formed by heat-treatment at 950°C and 1000°C in the glass with $x = 25$, i.e., *A phase*, could not be assigned to any phases in Gd$_2$O$_3$–B$_2$O$_3$–GeO$_2$ system reported so far. Therefore, the *A phase* is supposed to be a new compound in this system. Although it is quite difficult to examine the crystal structure of *A phase*, we speculated the structural features on the basis of the results in this study as possible.

The *A phase* would have a low-symmetric structure because of the complicated Raman spectra. In addition, the Raman bands around 800–900 cm^{-1} attributed to the vibration of GeO$_4$ unit, and at ~1040 cm^{-1} due to the presence of tetrahedral BO$_4$ unit with NBO (as mentioned above) also observed. Therefore, it is considered that the *A phase* consists of both the BO$_4$ unit with NBO and GeO$_4$ units. Furthermore, the SH intensity of *A phase*-crystallized sample obtained by the heat-treatment at 1000°C was evaluated to be $I_{2\omega}/I_{2\omega, \alpha\text{-quartz}}$~0.8. This strongly suggests that the *A phase* is noncentrosymmetric. The *A phase* is possibly formed between the T_{p1} and T_{p2} through the reaction between the B'-Gd$_2$Ge$_2$O$_7$ phase and B$_2$O$_3$ component in a residual amor-

phous phase, i.e.,

$$Gd_2Ge_2O_7 \text{ (B'-phase)} + B_2O_3 \text{ (in amorphous phase)} \rightarrow A\text{-phase.}$$
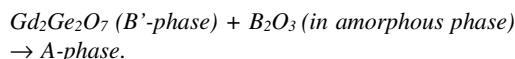
5. Summary and remarks

The effect of lanthanide (*Ln*) substitutions on physical properties, crystallization behavior and phase formation in the (25–x)La$_2$O$_3$·xGd$_2$O$_3$·25B$_2$O$_3$·50GeO$_2$ glasses, which are stoichiometry of the (La,Gd)BGeO$_5$, were clarified by means of the DTA, XRD and Raman techniques. Although the substitution of Gd^{3+} for La^{3+} provided no significant change in the physical properties, the drastic change in crystallization behavior and phase formation was confirmed by the substitution: The stillwellite-type phases singly crystallized in the glass with small quantity of Gd-substitution amount ($x = 0$–5). Further substitution of Gd^{3+} led to the formation of monoclinic phase with centrosymmetry (i.e. no SHG active).The Raman study in the glass and crystallized-glass samples revealed the closeness of glass structure to those of stillwellite-type LaBGeO$_5$ and the predominant-distribution of *Ln*$^{3+}$ in the vicinity of GeO$_4$ units in the (La,Gd)BGeO$_5$ glasses. In the glasses with $x = 20$ and 25, the high-pressure phase of B'-Gd$_2$Ge$_2$O$_7$ and the unidentified phase (i.e, *A*-phase) were precipitated by heat-treatment around T_{p1}. It was proposed that the *A*-phase consists of the BO$_4$ unit with non-bridging oxygen and GeO$_4$ unit, and is a new phase in the Gd$_2$O$_3$–B$_2$O$_3$–GeO$_2$ system.

Controlling of ferroelectric and nonlinear optical properties of the stillwellite-type glass-ceramics, and patterning of stillwellite phase in the corresponding glasses are achieved by the *Ln*-substitution for La^{3+} in the LaBGeO$_5$ glass.[10),18),19)] The *Ln*-substitution is quite important for the functional designs in the stillwellite-type glass-ceramics. However, the progressive substitution of smaller *Ln*$^{3+}$ in (La,Gd)BGeO$_5$ glasses leads to the decrease in crystallinity of the stillwellite phases and the formation of impurity (unidentified) phase, simultaneously. In addition, one can realize that the region of monoclinic phase tends to expand as the Gd^{3+} is largely substituted, as seen in Fig. 9. Therefore, it is necessary to suppress the formation of impurity and monoclinic phases if we desire to fabricate the ferroelectric or optical functional materials in the (La,*Ln*)BGeO$_5$ glass/glass-ceramics with high *Ln*$^{3+}$ concentration.

References

1) A. A. Kaminskii, A. V. Butashin, I. A. Maslyanizin, B. V. Mill, V. S. Mironov, S. P. Rozov, S. E. Sarkisov and V. D. Shigorin, *Phys. Stat. Sol. (a)*, **125**, 671–696 (1991).
2) S. Yu. Stefanovich, B. V. Mill and A. V. Butashin, *Sov. Phys. Crystallogr.*, **37**, 513–515 (1992).
3) A. Onodera, B. A. Strukov, A. A. Belov, S. A. Taraskin, H. Haga, H. Yamashita and Y. Uesu, *J. Phys. Soc. Jpn.*, **62**, 4311–4315 (1993).
4) E. L. Belokoneva, W. I. F. David, J. B. Forsyth and K. S. Knight, *J. Phys.: Condens. Matter*, **9**, 3503–3519 (1997).
5) I. Hrubá, S. Kamba, J. Petzelt, I. Gregora, Z. Zikmund, D. Ivannikov, G. Komandin, A. Volkov and B. Strukov, *Phys. Stat. Sol. (b)*, **214**, 423–439 (1999).
6) D. Jaque, J. Capmany, J. A. S. García, A. Brenier, G. Boulon and J. G. Solé, *Opt. Mater.*, **13**, 147–157 (1999).
7) V. N. Sigaev, S. Yu. Stefanovich, P. D. Sarkisov and E. V. Lopatina, *Glass Phys. Chem.*, **20**, 392–397 (1994).
8) V. N. Sigaev, S. Yu. Stefanovich, P. D. Sarkisov and E. V. Lopatina, *Glass Phys. Chem.*, **20**, 398–403 (1994).
9) S. Yu. Stefanovich and V. N. Sigaev, *Glass Phys. Chem.*, **21**, 253–262 (1995).
10) Y. Takahashi, A. Iwasaki, Y. Benino, T. Fujiwara and T. Komatsu, *Jpn. J. Appl. Phys.*, **41**, 3771–3777 (2002).
11) J. W. M. Verwey, D. V. D. Voort, G. J. Dirksen and G. Blasse, *J. Solid State Chem.*, **89**, 106–117 (1990).
12) A. A. Kaminskii, B. V. Bill, A. V. Butashin and V. D. Shigorin, *Inorg. Mater.*, **28**, 1643–1644 (1992).
13) Y. Takahashi, Y. Benino, V. Dimitrov and T. Komatsu, *J. Non-Cryst. Solids*, **260**, 155–159 (1999).
14) Y. Takahashi, Y. Benino, V. V. Dimitrov and T. Komatsu, *Phys. Chem. Glasses*, **41**, 225–228 (2000).
15) Y. Takahashi, Y. Benino, T. Fujiwara and T. Komatsu, *J. Appl. Phys.*, **89**, 5282–5287 (2001).
16) Y. Takahashi, K. Kitamura, Y. Benino, T. Fujiwara and T. Komatsu, *Mater. Sci. Eng. B*, **120**, 155–160 (2005).
17) Y. Takahashi, Y. Benino, T. Fujiwara and T. Komatsu, *Jpn. J. Appl. Phys.*, **41**, L1455–L1458 (2002).
18) Y. Takahashi, K. Saitoh, Y. Benino, T. Fujiwara and T. Komatsu, *J. Ceram. Soc. Japan*, Suppl., **112**, S1168–1172 (2004).
19) P. Gupta, H. Jain, D. B. Williams, J. Toulouse and I. Veltchev, *Opt. Mater.*, **29**, 355–359 (2006).
20) P. Gupta, H. Jain, D. B. Williams, T. Honma, Y. Benino and T. Komatsu, *J. Am. Ceram. Soc.*, **91**, 110–114 (2008).
21) V. Dimitrov and T. Komatsu, *J. Non-Cryst. Solids*, **249**, 160–179 (1999).
22) R. D. Shannon, *Acta Cryst. A*, **32**, 751–767 (1976).
23) A. Rulmont and P. Tarte, *J. Solid State Chem.*, **75**, 244–250 (1988).
24) H. Nasu, J. Matsuoka, O. Sugimoto, M. Kida and K. Kamiya, *J. Ceram. Soc. Japan*, **101**, 43–47 (1993).
25) C. Coussa, C. Martinet, B. Champagnon, L. Grosvalet, D. Vouagner and V. Sigaev, *J. Phys.: Condens. Matter*, **19**, 266220 (2007).
26) P. Pernice, A. Aronne, M. Catauro and A. Marrota, *J. Non-Cryst. Solid*, **210**, 23–31 (1997).
27) Y. Takahashi, K. Kitamura, S. Inoue, Y. Benino, T. Fujiwara and T. Komatsu, *Jpn. J. Appl. Phys.*, **44**, 7177–7181 (2005).
28) E. L. Belokonova, B. V. Mill, A. V. Butashin and A. A. Kaminskii, *Inorg. Mater.*, **27**, 1429–1436 (1991).
29) H. Verweij and J. H. J. M. Buster, *J. Non-Cryst. Solids*, **34**, 81–99 (1979).
30) T. Furukawa and W. B. White, *J. Chem. Phys.*, **95**, 776–784 (1991).
31) G. Bocquillon, J. Maugrion and J. Loriers, *Comptes Rendus C*, **287**, 5–8 (1978).
32) H. G. Kim, T. Komatsu, K. Shioya, K. Matusita, K. Tanaka and K. Hirao, *J. Non-Cryst. Solids*, **208**, 303–307 (1996).
33) S. K. Kurtz and T. T. Perry, *J. Appl. Phys.*, **39**, 3798–3813 (1968).